Accurate Pressure Calculation Method for CMP Modeling Using Fourier Analysis

Ruben Ghulghazaryan
Mentor Graphics Development Services
Yerevan, Armenia
e-mail:
ruben_ghulghazaryan@mentor.com

Suren Alaverdyan
Institute for Informatics and Automation Problems of NAS RA
Yerevan, Armenia
e-mail:
souren@ipia.sci.am

Davit Piliposyan
Mentor Graphics Development Services
Yerevan, Armenia
e-mail:
davit_piliposyan@mentor.com

ABSTRACT

Chemical-mechanical polishing/planarization (CMP) is one of the key processes used in electronic chip manufacturing. In CMP, a rotating wafer is pressed facedown onto a rotating polishing pad. A chemical "slurry" containing abrasive particles and chemical reagents is deposited on the pad during polishing, and flows between the wafer and the pad. The combined action of the polishing pad, abrasive particles, and chemical reagents results in material removal and planarization of the wafer surface.

In recent years, modeling of the CMP process has become critical for detection of planarity defects in chips before manufacturing. One of the key parameters affecting the surface planarization is the pressure, with which the wafer is pressed against the pad. Calculation of the pressure distribution across the wafer surface is crucial for modeling the CMP process. This pressure calculation typically uses contact mechanics methods that include solving an integral equation using fast Fourier (FFT) and inverse fast Fourier (IFFT) transforms. However, the kernel of the integral equation has singularities that lead to numerical instability.

In this paper, we propose a method to avoid numerical instabilities in pressure calculation by using an analytical expression for the Fourier transform of the kernel function.

Keywords

Chemical mechanical polishing, planarization, CMP, Fourier transform, information technology.

1. INTRODUCTION

Chemical-mechanical polishing/planarization (CMP) is an electronic chip manufacturing process for removing excess conductive and dielectric materials from a silicon wafer to smooth out and flatten the wafer surface using the combined action of chemical reactions and mechanical forces (Fig. 1). It uses a chemical slurry in conjunction with a polishing pad to remove material and even out irregular topography for wafer surface planarization. CMP results are very sensitive to the applied pressure, slurry chemistry, and the pattern printed on the wafer, which may result in dishing of metal lines and erosion of dielectrics.

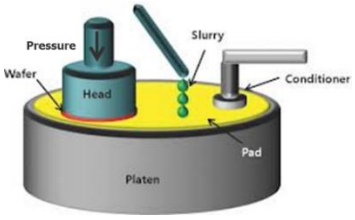

Figure 1. Schematic view of CMP process.

Numerous wafer-scale and feature-scale CMP models have been proposed to predict the evolution of the wafer surface during the polishing process. Moving to new technology nodes that require high-k metal gate (HKMG) technology with additional CMP steps, the high cost of lithography due to double and triple patterning, strong depth of focus (DOF) requirements, and improving the accuracy of CMP models have all increased interest in CMP modeling [1-3].

The front end-of-line (FEOL) and back end-of-line (BEOL) are the two main segments in the fabrication of integrated circuits (ICs). The FEOL process is the first part of IC fabrication. It includes all the process steps necessary to build the substrate architecture, including the architecture for the electrical isolation structures, transistors, capacitors, resistors, etc. The BEOL process connects all these integrated devices, forming the necessary logic and memory circuits. Both of these segments depend strongly on the deposition of layers of different materials, using a variety of deposition technologies to deposit oxides, glasses, conductors, and nitrides.

The post-deposition surface profile is used as input for CMP modeling. Normally, the material removal rate during polishing is proportional to the applied pressure (Preston's law). However, even with advanced deposition processes, the post-deposition profile of a patterned wafer is non-uniform. It may contain large variations that can affect surface planarity after CMP. Thus, calculation of the pressure distribution over the chip area is crucial for accurately modeling the surface profile of the chip after CMP. Recently, a neural network-based full-chip deposition model for predicting the post-deposition profile surface was proposed [4].

In this paper, we focus on the problem of accurate pressure calculation for CMP modeling. The pressure distribution over chip surface is one of the key factors affecting the surface planarity, non-local interactions, and long-range effects during CMP. Thus, accurate calculation of pressure distribution over chip area is a question of primary interest.

We concentrate on the pressure calculation method based on Hertz contact theory and the Chekina model [5]. This model assumes the pad is a massive elastic body, the surface of which is flat, and the wafer is a rigid body. The calculations involve application of fast Fourier (FFT) and inverse fast Fourier (IFFT) transforms for pressure calculation using pad displacement. Typically, the kernel of the integral equation has singularities, which are avoided by adding a constant parameter to the kernel function. This generates numerical instabilities and slows down the convergence of the algorithm. Using theorems and ideas discussed in this paper, we were able to derive an analytical expression of the kernel function Fourier transform and avoid the appearance of singularities.

2. SUPPORTING THEOREMS

The Fourier and inverse Fourier transforms of the function f(x) have the following forms

$$F(\omega) = \frac{1}{\sqrt{2\pi}} \int_{-\infty}^{\infty} f(x)\, e^{-i\omega x} dx\,, \qquad f(x) = \frac{1}{\sqrt{2\pi}} \int_{-\infty}^{\infty} F(\omega)\, e^{i\omega x} d\omega.$$

For simplicity, we denote Fourier and inverse Fourier transforms as $\Phi(\cdot)$ and $\Phi^{-1}(\cdot)$.

Theorem 1 (Convolution): The Fourier transform of convolution of two functions is equal to the product of Fourier transforms of those two individual functions.

$$\Phi(f * g) = \sqrt{2\pi}\Phi(f)\Phi(g), \tag{1}$$

where

$$(f * g)(x) = \int_{-\infty}^{\infty} f(x-s)g(s)ds. \tag{2}$$

Lemma (Riemann-Lebesgue): If $f(x) \in L^1$ then

$$\lim_{|\omega|\to\infty} \Phi(\omega) = 0. \tag{3}$$

Proof: We will only show that the Fourier transform $\Phi(f)$ of the function f (x) is limited

$$|\Phi(\omega)| = \frac{1}{\sqrt{2\pi}} \left| \int_{-\infty}^{\infty} f(x)\, e^{-i\omega x} dx \right|,$$

$$\frac{1}{\sqrt{2\pi}} \left| \int_{-\infty}^{\infty} f(x)\, e^{-i\omega x} dx \right| \le \frac{1}{\sqrt{2\pi}} \int_{-\infty}^{\infty} |f(x)| \left| e^{-i\omega x} \right| dx,$$

$$\frac{1}{\sqrt{2\pi}} \int_{-\infty}^{\infty} |f(x)| \left| e^{-i\omega x} \right| dx = \frac{\|f\|}{\sqrt{2\pi}} < \infty.$$

Theorem 2: If function $f(x) \in L^1$ and its derivative $f'(x) \in L^1$, then the Fourier transform of the derivate $f'(x)$ has the following form:

$$\frac{1}{\sqrt{2\pi}} \int_{-\infty}^{\infty} f'(x) e^{-i\omega x} dx = i\omega\, F(\omega). \tag{4}$$

From the *Riemann-Lebesgue Lemma* and *Theorem 2* the following condition follows:

$$|F(\omega)| \le \frac{c}{|\omega|}, \tag{5}$$

where *c* is a constant number.

Theorem 3: If the Fourier transform of the function $K(x,y) = \frac{1}{\sqrt{x^2+y^2}}$ satisfies the condition

$$\int_a^b \int_c^d |K(x,y)|^2 dxdy < \infty, \tag{6}$$

then for K(x,y) the following equation is true

$$\lim_{N\to\infty} \frac{1}{4\pi^2} \int_a^b \int_c^d |K(x,y) - K_N(x,y)|^2 dxdy = 0,$$

where $K_N(x,y)$ is the nth partial sum of the $K(x,y)$ function Fourier series.

3. PRESSURE CALCULATION

Suppose a rigid wafer is pressed against the elastic flat surface of a polishing pad with applied pressure P_0 (Fig. 2). Since the wafer surface is not flat, the polishing pad deforms, leading to the appearance of pad displacements. The line ***a*** is the reference line, with respect to which the displacements are calculated. Let's define the perturbation pad displacements w_{pad} as the distance between the top of the pad surface and the reference line ***a*** (dashed arrow line in Fig. 2), and the wafer profile height w_{wafer} as the distance between the top of the surface of the wafer and the reference line ***a*** (solid arrow line in Fig. 2).

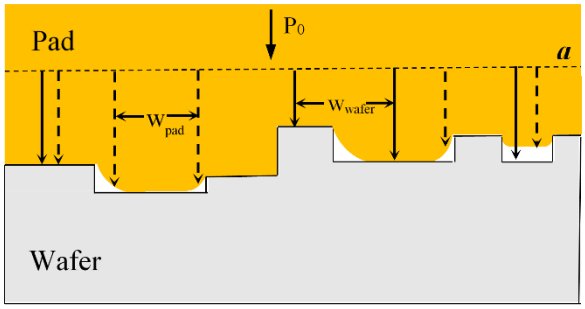

Figure 2. Wafer-pad contact surface.

The relation between the displacements of the surface at each point w(x, y) and the contact pressure p(x, y) can be obtained from the Hertz equation, which is a Fredholm equation of the first kind

$$w(x,y) = \mathrm{k_c} \int_a^b \int_c^d \frac{p(\xi,\eta)}{\sqrt{(x-\xi)^2 + (y-\eta)^2}} d\xi d\eta, \tag{7}$$

where $k_c = (1-\nu)/\pi E$ is related to Poisson's ratio ν. This equation can be considered as a convolution of the pressure P(x,y) and the kernel function K(x,y),

$$w(x,y) = k_c\, (p(\xi,\eta) * K(x,y)), \tag{8}$$

where

$$K(x,y) = \frac{1}{\sqrt{x^2+y^2}}. \tag{9}$$

According to the *convolution Theorem 1* for the Fourier transforms of the displacements we have

$$\Phi\big(w(x,y)\big) = k_c \Phi\big(p(\xi,\eta)\big) \times \Phi\big(K(x,y)\big). \tag{10}$$

From (10) using Fourier analysis, the pressure-displacement relation can be written in the following form:

$$p(x,y) = \frac{1}{k_c} \Phi^{-1}\left(\frac{\Phi\big(w(x,y)\big)}{\Phi\big(K(x,y)\big)} \right). \tag{11}$$

The function $K(x,y)$ has a singularity at the start point of the coordinate system and is replaced with

$$K(x,y) = \frac{1}{\sqrt{x^2+y^2+\varepsilon}}, \tag{12}$$

where ε is a small number. The introduction of ε solves the singularity problem; however, it also generates numerical instabilities and slows down the convergence rate of the pressure calculation algorithm.
Using the *Riemann-Lebesgue Lemma* and *Theorem 2*, an analytic expression for the Fourier transform of the kernel (8) can be derived. The analytic expression of the kernel function provides better accuracy and improves algorithm stability and convergence rate.

Algorithm description:

- Assume that the pad is in contact with the wafer everywhere. This means that the pad perturbation displacement w_{pad} is equal to the known profile height w_{wafer}.
- Using equation (6) and the analytical expression for a Fourier transform of the kernel function, calculate the pad pressure in each cell.

$$p_{pad}(x,y) = \frac{1}{k_c}\Phi^{-1}\left(\frac{\Phi\left(w_{pad}(x,y)\right)}{\Phi\left(K(x,y)\right)}\right)\Bigg|_{w_{pad}=w_{wafer}} . \quad (13)$$

- For each cell, check that the contact pressure is positive.
$$P_0 - p_{pad} \geq 0. \quad (14)$$
- If the contact pressure is negative, it means that the pad is not in contact with the wafer in that cell. For that cell, decrease the pad displacement value w_{pad} by a fixed step δ_D and recalculate the pressure distribution.
- Repeat the procedure until constraint (14) is satisfied for all cells.

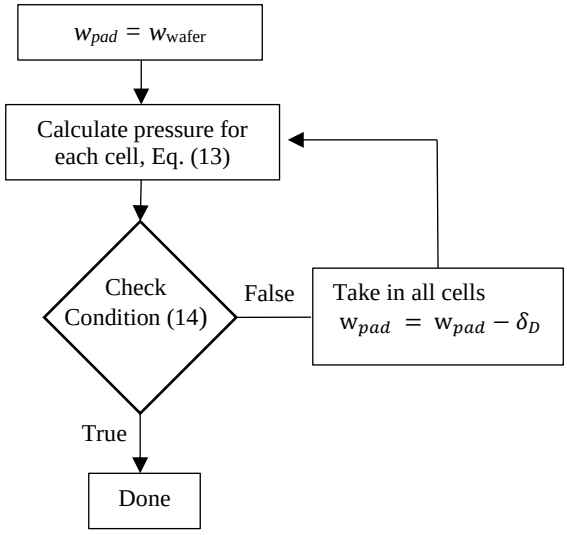

- Finally, calculate the actual pressure on the wafer surface as follows:

$$P = \begin{cases} P_0 - p_{pad} & w_{pad} = w_{wafer} \\ 0 & w_{pad} < w_{wafer} \end{cases} .$$

4. NUMERICAL RESULTS

The algorithm was tested on several profile patterns (Figs. 3-6). The results show that the profile of the contact pressure is in agreement with expectations. All numerical computations were done with the same pad stiffness value ($1/k_c$= 125200 kPa) and applied pressure (9.3kPa).

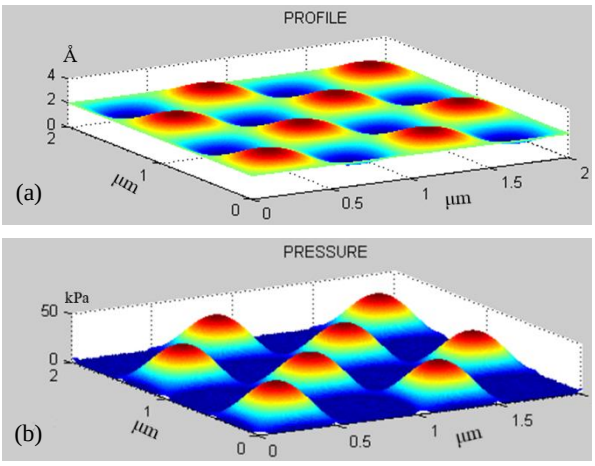

Figure 3. (a) Wafer surface profile for the sinusoidal shapes, (b) Pad pressure distribution for sinusoidal surface case.

First we considered a wafer surface profile with evenly distributed sinusoidal shapes (Fig. 3(a)). Here the pressure distribution takes the maximum values on the profile bumps peaks, which is expected for the considered surface pattern (Fig. 3(b)).

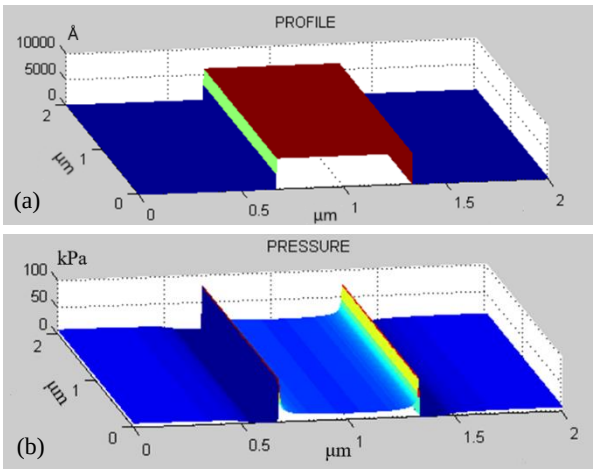

Figure 4. (a) Wafer surface profile for a single prism; (b) Pad pressure distribution for a single prism.

In Fig. 4(a) and Fig. 5(a), profiles of patterns with constant length single and multiple prismatic patterns are considered. The pressure distribution maximum values are concentrated on the edges of the profile bumps over prismatic patterns for both the structure containing single (Fig. 4(b)) or multiple prisms (Fig. 5(b)). Such behavior is in agreement with expectations.

In Fig. 6(a), structures with varying size prismatic patterns are considered. In Fig. 6(b), the distribution of pressure over the patterns is shown. We see that the maximum pressure values are achieved on the corners of the short prisms, and pressure on the edges of the prisms are higher than at the center parts. The predicted pressure distribution is in agreement with expectations. These and other patterns were tested with the proposed method and all of them showed correct physical behavior. This confirms that the method predicts correct pressure distribution and may be used for CMP modeling.

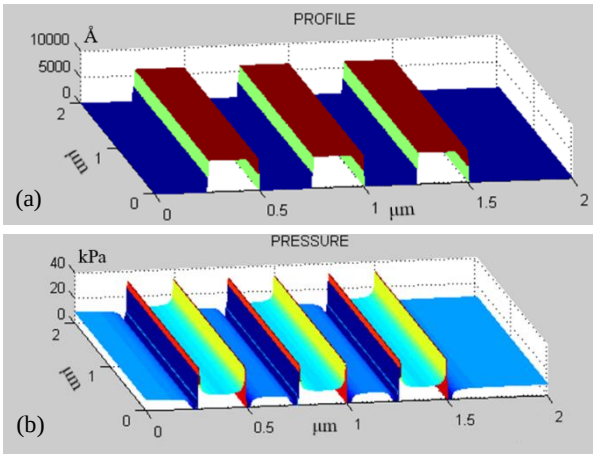

Figure 5. (a) Wafer surface profile for prismatic shapes separated by the same distance; (b) Pad pressure distribution for a multiple prisms pattern.

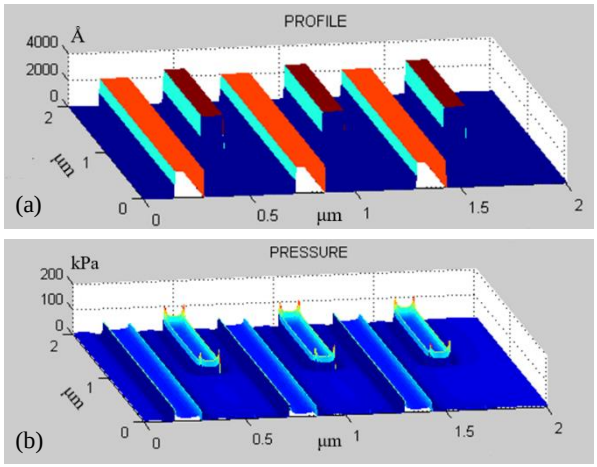

Figure 6. (a) Wafer surface profile for multiple prismatic shapes of different lengths; (b) Pad pressure distribution.

In the next series of experiments, we investigated the algorithm convergence and its effect on the runtime. We observed that removing singularity of the kernel function by using an analytical expression for the Fourier transform of the kernel function may decrease the number of iterations for pressure distribution convergence by 10-30% and improve the runtime, in some cases by 30%.

5. CONCLUSION

CMP modeling is crucial for the detection of planarity defects in chips before manufacturing. Pad pressure distribution over chip area plays a critical role during polishing. Namely, pressure distribution is responsible for long-range pattern interactions or long-range effects in CMP, and highly affects erosion of dielectrics and dishing of wide metal lines after polishing. Contact mechanics methods are typically used to calculate the pressure distribution, which involve computations of FFT and IFFT of the kernel function with singularities. Due to new technology developments and the increase of the number of patterns printed on wafers, the size of wafers are increasing. Thus, faster and stable algorithms with higher rates of convergence are needed for pressure distribution calculation for CMP modeling.

In this paper, we discussed a new method for pressure calculation based on an analytical expression for a Fourier transform of the singular kernel function of pressure distribution integral equation. The new method provides much more accurate numerical results, and improves pressure calculation algorithm convergence and runtime.

6. ACKNOWLEDGEMENT

This work is done under the support of a joint collaboration project between Mentor, a Siemens business and The Institute for Informatics and Automation Problems of National Academy of Science of Armenia. The authors would like to express their appreciation to Shelly Stalnaker for her editorial assistance in the preparation of this paper.

REFERENCES

[1] D. Zhao, X. Lu, "*Chemical mechanical polishing: Theory and experiment*" Friction, pp 306-326, 2013

[2] R. Ghulghazaryan, J. Wilson and A. Abouzeid, "*FEOL CMP Modeling: Progress and Challenges*" International Conference on Planarization/CMP Technology (ICPT), pp 1-4, Chandler, USA, 2015.

[3] R. Ghulghazaryan, J. Wilson, N. Takeshita, "*CMP Model Building and Hotspot Detection by Simulation*" Proceedings of 158th Meeting of Planarization CMP Committee, p. 55, Nagoya, Japan 2017.

[4] R. Ghulghazaryan, D. Piliposyan, J. Wilson, "*Application of Neural Network-Based Oxide Deposition Models to CMP Modeling*" ECS Journal of Solid State Science and Technology, pp 3154-3162, 2019.

[5] O. G. Chekina, L. M. Keer, "*Wear-Contact Problems and Modeling of Chemical Mechanical Polishing*" Journal of The Electrochemical Society, vol. 145, no. 6, pp. 2100-2106, 1998.